



OPEN ACCESS

EDITED BY

Nan Zhang,
Harbin Medical University, China

REVIEWED BY

Pan Li,
Southern Medical University, China
Xia Chen,
Southern Medical University, China

*CORRESPONDENCE

Zhuna Wu
wuzhuna@aliyun.com

[†]These authors have contributed equally to this work and share first authorship

SPECIALTY SECTION

This article was submitted to Cancer Immunity and Immunotherapy, a section of the journal Frontiers in Oncology

RECEIVED 30 October 2022

ACCEPTED 16 November 2022

PUBLISHED 30 November 2022

CITATION

Ke Y, You L, Xu Y, Wu D, Lin Q and Wu Z (2022) DPP6 and MFAP5 are associated with immune infiltration as diagnostic biomarkers in distinguishing uterine leiomyosarcoma from leiomyoma.

Front. Oncol. 12:1084192.

doi: 10.3389/fonc.2022.1084192

COPYRIGHT

© 2022 Ke, You, Xu, Wu, Lin and Wu. This is an open-access article distributed under the terms of the [Creative Commons Attribution License \(CC BY\)](https://creativecommons.org/licenses/by/4.0/). The use, distribution or reproduction in other forums is permitted, provided the original author(s) and the copyright owner(s) are credited and that the original publication in this journal is cited, in accordance with accepted academic practice. No use, distribution or reproduction is permitted which does not comply with these terms.

DPP6 and MFAP5 are associated with immune infiltration as diagnostic biomarkers in distinguishing uterine leiomyosarcoma from leiomyoma

Yumin Ke^{1†}, LiuXia You^{2†}, YanJuan Xu³, Dandan Wu⁴, Qiuya Lin¹ and Zhuna Wu^{1*}

¹Department of Gynecology and Obstetrics, The Second Affiliated Hospital of Fujian Medical University, Quanzhou, Fujian, China, ²Department of Clinical Laboratory, The Second Affiliated Hospital of Fujian Medical University, Quanzhou, Fujian, China, ³Department of Pathology, The Second Affiliated Hospital of Fujian Medical University, Quanzhou, Fujian, China, ⁴Department of Gynecology, The First Hospital of Quanzhou Affiliated to Fujian Medical University, Quanzhou, Fujian, China

Objective: Uterine leiomyosarcoma (ULMS) is the most common subtype of uterine sarcoma and is difficult to discern from uterine leiomyoma (ULM) preoperatively. The aim of the study was to determine the potential and significance of immune-related diagnostic biomarkers in distinguishing ULMS from ULM.

Methods: Two public gene expression profiles (GSE36610 and GSE64763) from the GEO datasets containing ULMS and ULM samples were downloaded. Differentially expressed genes (DEGs) were selected and determined among 37 ULMS and 25 ULM control samples. The DEGs were used for Gene Ontology (GO), Kyoto Encyclopaedia of Genes and Genomes (KEGG) and Disease Ontology (DO) enrichment analyses as well as gene set enrichment analysis (GSEA). The candidate biomarkers were identified by least absolute shrinkage and selection operator (LASSO) and support vector machine recursive feature elimination (SVM-RFE) analyses. The receiver operating characteristic curve (ROC) was applied to evaluate diagnostic ability. For further confirmation, the biomarker expression levels and diagnostic value in ULMS were verified in the GSE9511 and GSE68295 datasets (12 ULMS and 10 ULM), and validated by immunohistochemistry (IHC). The CIBERSORT algorithm was used to calculate the compositional patterns of 22 types of immune cells in ULMS.

Result: In total, 55 DEGs were recognized *via* GO analysis, and KEGG analyses revealed that the DEGs were enriched in nuclear division, and cell cycle. The recognized DEGs were primarily implicated in non-small cell lung carcinoma and breast carcinoma. Gene sets related to the cell cycle and DNA replication were activated in ULMS. *DPP6* and *MFAP5* were distinguished as diagnostic

biomarkers of ULMS (AUC = 0.957, AUC = 0.899, respectively), and they were verified in the GSE9511 and GSE68295 datasets (AUC = 0.983, AUC = 0.942, respectively). The low expression of *DPP6* and *MFAP5* were associated with ULMS. In addition, the analysis of the immune microenvironment indicated that resting mast cells were positively correlated with *DPP6* and *MFAP5* expression and that eosinophils and M0 macrophages were negatively correlated with *DPP6* expression ($P < 0.05$).

Conclusion: These findings indicated that *DPP6* and *MFAP5* are diagnostic biomarkers of ULMS, thereby offering a novel perspective for future studies on the occurrence, function and molecular mechanisms of ULMS.

KEYWORDS

diagnostic biomarkers, machine-learning, *DPP6*, *MFAP5*, immune infiltration, uterine leiomyosarcoma

Introduction

Uterine leiomyosarcoma (ULMS) is a rare but aggressive tumor subtype, accounting for approximately 1% of all uterine malignancies (1). ULMS is the most common subtype of uterine sarcoma and originates from the smooth muscles of the myometrium. In the past several decades, the prognosis of ULMS patients has not changed with an overall 5-year survival rate of only 15%-25% (2). Currently, complete surgical resection is the primary treatment for early-stage ULMS (3), and chemotherapy is regarded as the standard therapy for advanced or metastatic ULMS (4, 5), but with an estimated recurrence rate of approximately 50 to 70% (6). ULMS constitutes a sizable proportion of uterine cancer deaths (7). Additionally, compared to other gynecological malignancies, ULMS etiology, pathogenesis and earlier diagnosis are poorly understood. Considering that ULM can currently be treated with minimally invasive surgery, it is important to discern ULMS from ULM preoperatively to avoid disseminated spread by laparoscopic morcellation or delayed diagnosis with conservative treatment (8, 9). Considering that ULMS has a high trend towards local recurrence, metastasis and poor prognosis, the misdiagnosis of a ULMS for a leiomyoma may lead to therapy delays and higher morbidity (10, 11).

ULMS patients generally present with abnormal vaginal bleeding, pelvic pain and palpable pelvic mass. Because these symptoms resemble ULM, particularly degenerated ULM, it is difficult to discern ULMS and ULM by pelvic ultrasound and MRI preoperatively (12). Postoperative pathological diagnosis is currently the only available method to distinguish the two tumor conditions. A meta-analysis containing 133 studies has indicated that undiagnosed ULMS estimated to be approximately 1 in

2000 surgeries for presumed ULM (13). It is well known that tumor-associated immunity plays a vital role in the occurrence, development and metastasis of tumors (14). The recent development of integrated microarray technology with bioinformatics analysis may allow identification of novel genes that might act as diagnostic and prognostic biomarkers in cancers (15, 16). Definitive molecular diagnosis added to histopathological diagnosis should be considered to decrease the risk of misdiagnosis. Verification of highly novel diagnostic biomarkers for ULMS related to immune cell infiltration will further improve the diagnostic accuracy of ULMS.

Herein, the aim of this study was to identify novel diagnostic immune-related genes for ULMS. Machine-learning algorithms and logistic regression were used to verify diagnostic biomarkers of ULMS. Furthermore, CIBERSORT was applied to compute the quotas of infiltrating immune cells between ULMS and ULM samples. Finally, the correlation among the recognized diagnostic biomarkers and infiltrating immune cells was explored to offer a foundation for further research.

Materials and methods

Microarray data processing and identification of DEGs

First, we obtained datasets (GSE36610 and GSE64763 as the training group; and GSE9511 and GSE68295 as the testing group) from the GEO database (<https://www.ncbi.nlm.nih.gov/gds>) (Table 1). The background correction and normalization of raw data were processed by the limma package of R software (<http://www.bioconductor.org/>). Two datasets were merged into

TABLE 1 GEO database data of preeclampsia mRNA expression profile.

Dataset ID	Platform	leiomyosarcoma	leiomyoma
Train group			
GSE36610	GPL7363-11635	12	0
GSE64763	GPL571-17391	25	25
Test group			
GSE9511	GPL80-30376	9	7
GSE68295	GPL6480-9577	3	3

a metadata cohort, and the batch effect was removed with the SVA package of R software (17). Genes with $|\log$ fold change (FC)| > 2 and adjusted $P < 0.05$ were defined as DEGs.

Functional enrichment of DEGs

The DEGs were analyzed using the clusterProfiler, org.Hs.eg.db, enrichplot and ggplot2 packages of R software for GO and KEGG analyses. The clusterProfiler and DOSE packages of R software were used to perform DO analyses on DEGs. GSEA was conducted to recognize the most important feature between the ULMS and ULM groups. “c2.cp.kegg.v7.4.symbols.gmt” was applied as the reference gene set from the Molecular Signatures Database (MSigDB). $P < 0.05$ was considered a significant enrichment.

Screening candidate biomarker for diagnosis of ULMS

We applied two machine-learning algorithms to increase the prediction accuracy. LASSO is a regression-based analysis that scrutinizes variable selection and regularization in ULMS models. The glmnet package of R software was applied to perform LASSO regression analysis on the identification of DEGs correlated with the discernment between ULMS and ULM. The support vector machine (SVM) is an efficient and widely applied supervised machine-learning algorithm for disease classification and regression tasks (18). Consequently, we screened the overlapping genes by conjugating LASSO and SVM-RFE followed by verification using the GSE9511 and GSE68295 datasets.

Significance of diagnostic biomarkers in ULMS

We obtained mRNA expression data from 37 ULMS and 25 ULM samples, which were applied to create ROC curves to verify the biomarker predictive ability. The area under the ROC curve (AUC) was utilized to determine the ability of diagnosis in distinguishing ULMS from ULM samples followed by verification using the GSE9511 and GSE68295 datasets.

Evaluating the level of immune infiltration

We downloaded a gene signature matrix with interpretation, known as the 22 immune cell (LM22) matrix with 1,000 permutations from CIBERSORT (<http://cibersort.stanford.edu/>) (19). The CIBERSORT algorithm was applied to quantify the proportion of 22 infiltrating immune cells in the tissue using the expression of 547 immune-related genes. The corrpilot package in R software was applied to conduct the correlation and visualization of 22 types of infiltrating immune cells. The vioplot package in R software was used to study the infiltration of immune cells between the ULMS and ULM groups. Pearson correlation analysis was applied to explore the selected diagnostic biomarkers correlated with the levels of infiltrating immune cells.

Patient and tissue samples

Twenty-six paraffin-embedded ULMS and twenty-three ULM specimens were diagnosed at The Second Affiliated Hospital of Fujian Medical University (Fujian, China) from September 2010 to February 2022. The main treatment of all patients underwent hysterectomy with bilateral adnexal resection. The research was approved by the Research Ethics Committee of The Second Affiliated Hospital of Fujian Medical University prior to the study.

Immunohistochemistry

IHC staining was operated as previously described (20). The primary antibodies included anti-DPP6 (Bioss, Beijing), anti-MFAP5 (Proteintech, USA). The proportion of DPP6 and MFAP5 staining intensity was scored as follows: negative = 0; light yellow = 1; brownish yellow = 2; or tan = 3. The staining was scored as follows: less than 1/3 = 1; between 1/3 and 2/3 = 2; or more than 2/3 = 3. The final score for DPP6 and MFAP5 expression was calculated by multiplying the 2 scores. The slides were classified to low and high expression group, corresponding to scores of <3 or ≥ 3 , respectively. The histopathological diagnosis of the patients included in our study was established by two pathologists specialized in Gynecologic Oncology.

Statistical analysis

We utilized R software to conduct (v.4.1.1) all statistical analyses. We used the Mann–Whitney U test to compare the different groups. LASSO regression, SVM algorithm, ROC curve, Pearson’s correlation and unpaired t test were used as described above. Differences with $P < 0.05$ were considered statistically significant for all statistical analyses.

Result

Study procedure

The analysis procedure of the present is shown in Figure 1. The transcriptome RNA-seq data were downloaded from the GEO database. We identified the DEGs between the ULMS and ULM group. DEGs were analyzed using the GO, KEGG and DO analyses as well as GSEA. LASSO and SVM-RFE were used to select the candidate overlapping genes, and ROC curves were applied to check the predictive ability of biomarkers, which was

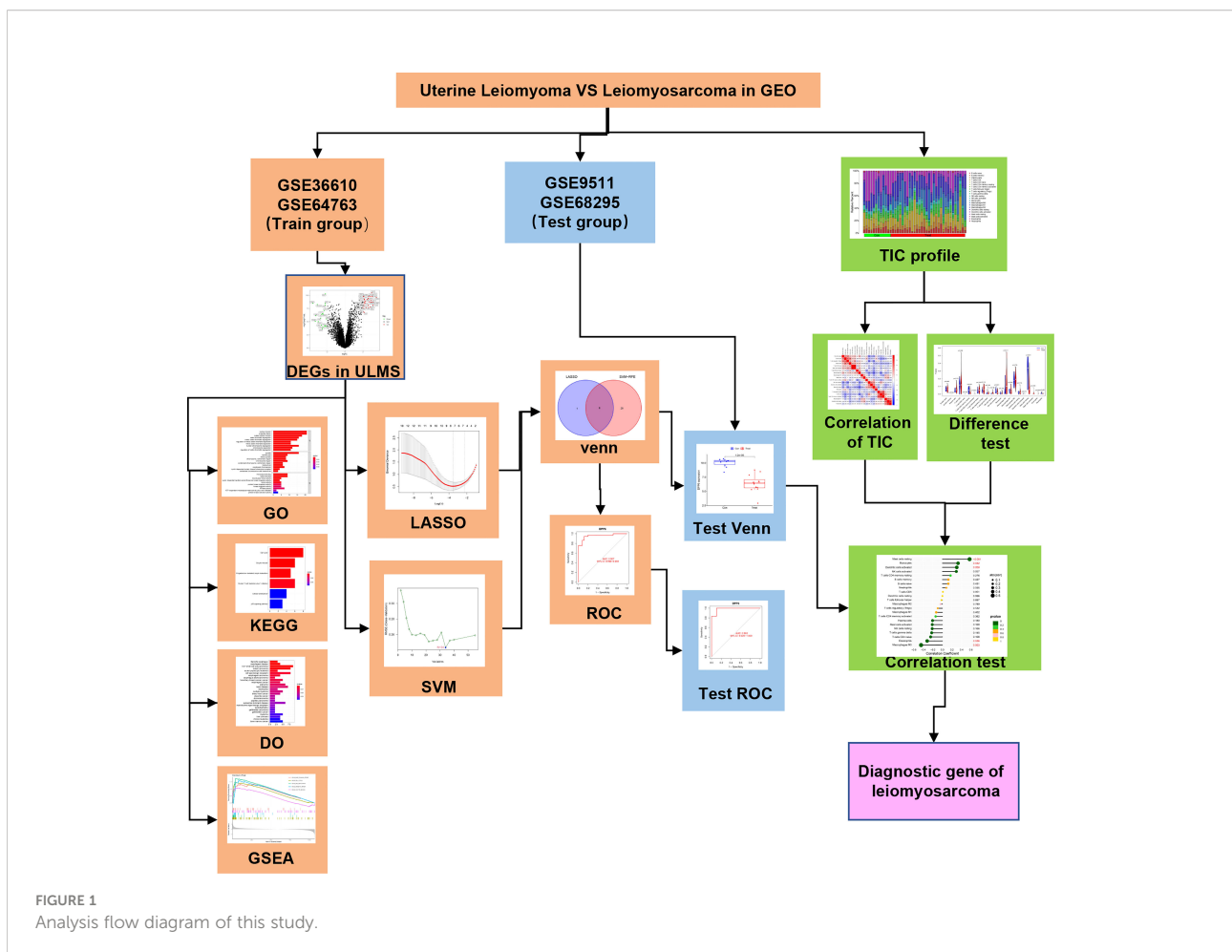
further verified in the GSE9511 and GSE68295 datasets. The compositional patterns of 22 immune cells were calculated using CIBERSORT in ULMS. Finally, correlation analysis among the diagnostic markers and infiltrating immune cells was performed.

Identification of DEGs in ULMS

The present study utilized two datasets (GSE36610, GSE64763) and included 37 ULMS and 25 ULM samples. We identified 55 DEGs by comparing ULMS and ULM (Figure 2A). Among these DEGs, 21 genes were significantly downregulated, and 34 genes were significantly upregulated. The volcano plot in Figure 2B shows the distribution of the top 50 DEGs in ULMS and ULM.

Correlation and functional enrichment analysis

The GO analysis indicated that the DEGs mainly participated in chromosome segregation and the cell cycle



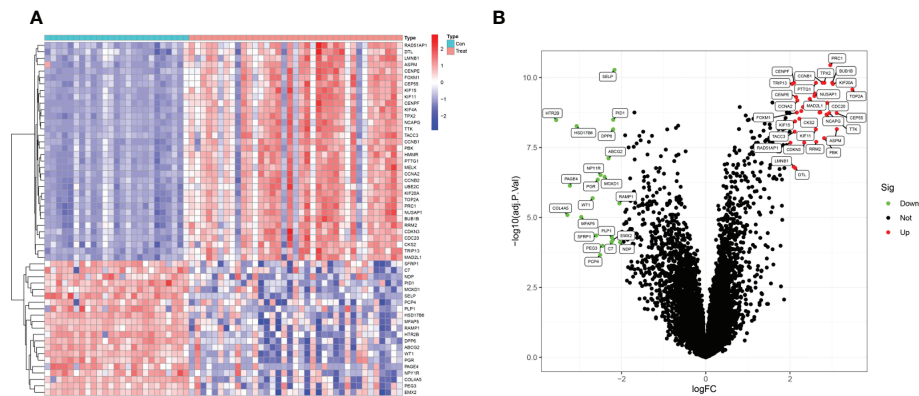


FIGURE 2

Identification of DEGs. (A) Heatmap plots of 55 DEGs between ULMS and ULM samples from GEO database. Row name of heatmap is the gene name, and column name is the ID of samples which not shown in plot. The colors from red to blue represent expression level from high to low in the heatmaps. (B) Volcano plots of top 50 DEGs between ULMS and ULM samples. The red dots in the volcano plots represent up-regulation, the green dots represent down-regulation and black dots represent genes without differential expression.

(Figure 3A). In addition, KEGG analysis showed enrichment of the cell cycle and immune-related pathways, such as HTLV-1 infection way (Figure 3B). The DO enrichment showed that DEGs were mostly related to solid malignant tumors and haematological malignancies (Figure 3C). The GSEA results revealed negative enrichment in cell adhesion and the Wnt signalling pathway in ULM (Figure 3D, Table S1) as well as positive enrichment in the cell cycle, DNA replication and mismatch repair in ULMS (Figure 3E, Table S2). These results indicated that mismatch repair, related immunity and the cell cycle play vital roles in ULMS.

Verification and validation of diagnostic biomarkers

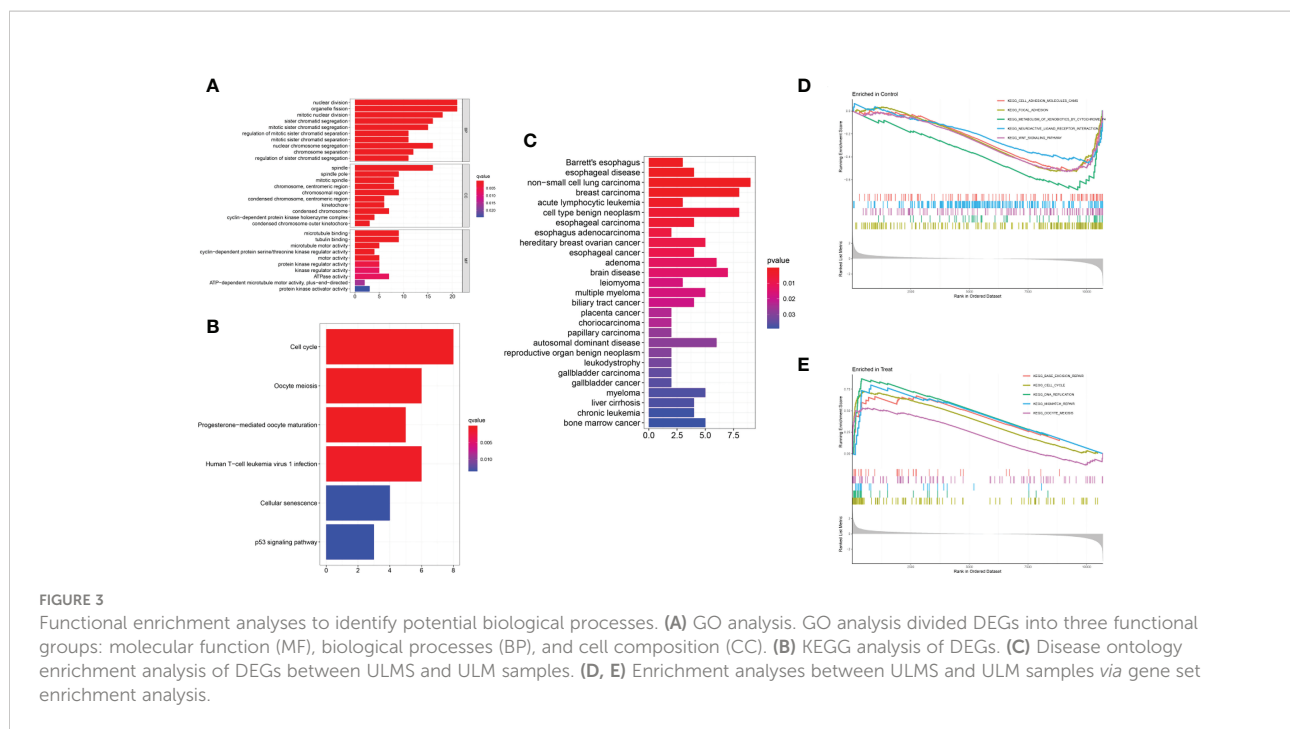
We employed the LASSO and SVM-RFE algorithm methods to select potential biomarkers. We identified 7 DEGs as diagnostic biomarkers using LASSO regression for ULMS (Figure 4A), and we verified 34 DEGs using the SVM-RFE (Figure 4B). When integrating both algorithms, six overlapping candidate genes (*PRC1*, *SELP*, *PID1*, *DPP6*, *MFAP5* and *HSD17B6*) were selected (Figure 4C). In addition, with the purpose of producing more dependable and exact DEGs, we verified the expression levels of six DEGs using the GSE9511 and GSE68295 datasets. The *DPP6* and *MFAP5* expression levels in ULMS samples were significantly lower than those in the ULM group (Figures 5A, B; $P < 0.05$). However, *SELP* gene expression was not significantly different between the two groups (Figure 5C). Subsequently, we investigated the latent ability of the two identified DEGs as diagnostic biomarkers utilizing a logistic regression algorithm.

Effectiveness of diagnostic biomarkers in ULMS

The ability of the two diagnostic biomarkers indicated good diagnostic value in early discernment of ULMS as the AUC values of the *DPP6* and *MFAP5* genes were 0.957 and 0.899, respectively (Figure 6A). Subsequently, a persuasive screening capacity was verified in the GSE9511 and GSE68295 datasets with AUC values of 0.983 in *DPP6* and 0.942 in *MFAP5* (Figure 6B). We assessed the expression of *DPP6* and *MFAP5* across ULMS and ULM tissues *via* immunohistochemistry and found that low expression of *DPP6* and *MFAP5* were associated with ULMS. *DPP6* was expressed in the cytoplasm, *MFAP5* was expressed in the stroma. (Figures 6C, D; $P < 0.05$). The above results indicating that the *DPP6* gene and *MFAP5* had a higher diagnostic capacity.

DPP6 and *MFAP5* genes correlate with the percentage of immune cell infiltration

Next, we verified the correlation of the *DPP6* and *MFAP5* genes with immune cell infiltration. We determined the proportions of 22 immune cells in the ULMS and ULM samples using the CIBERSORT algorithm (Figures 7A, B). The components of immune cells in the ULMS vs. ULM group were explored. The ratios of resting CD4+ memory T cells ($P = 0.023$), activated NK cells ($P = 0.031$) and resting mast cells ($P < 0.001$) in the ULMS group were markedly lower than those in the ULM group. However, the ratio of M0 macrophages ($P = 0.011$) was significantly higher in ULMS compared to ULM (Figure 7C).



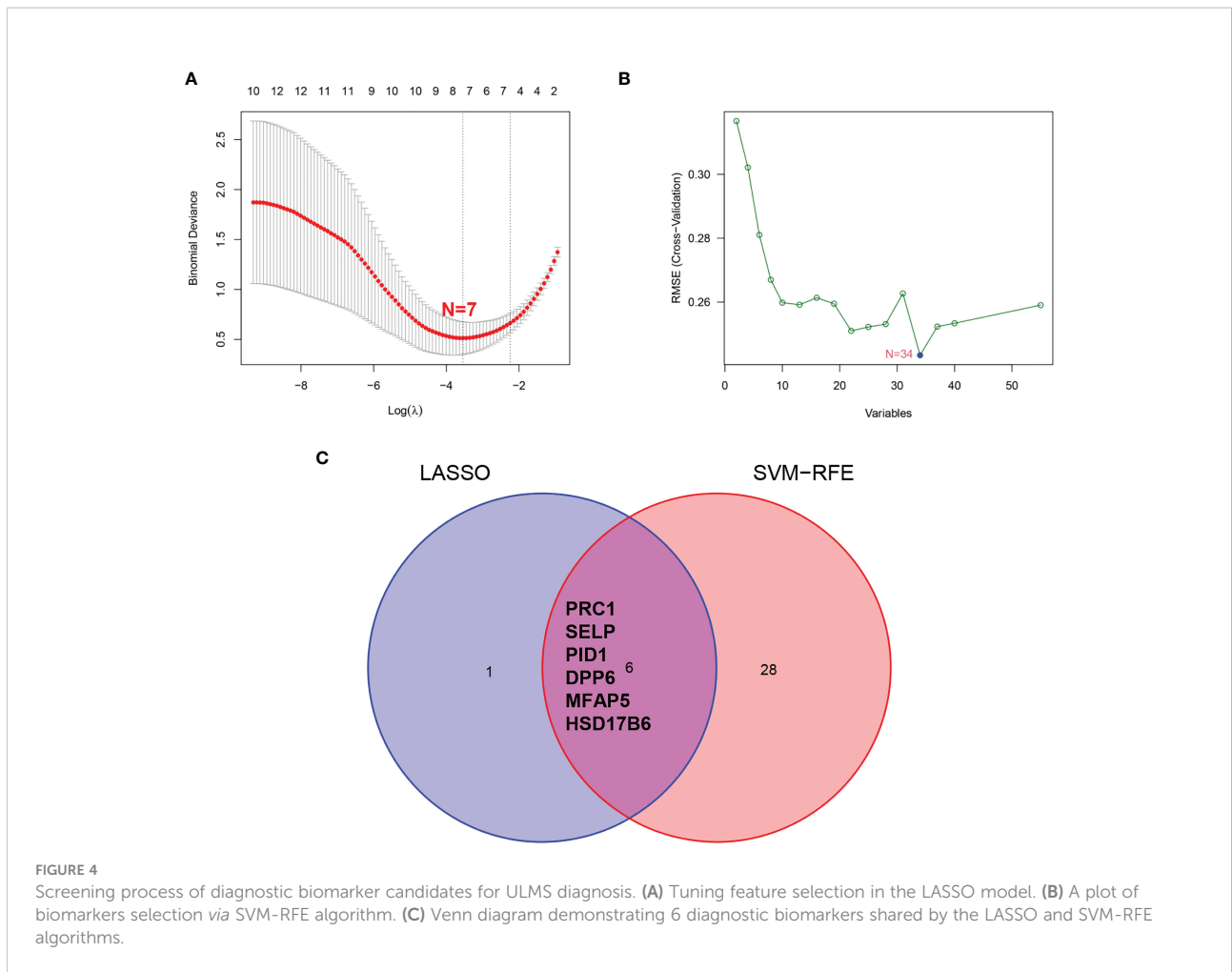
Furthermore, we studied the relationship between the *DPP6* and *MFAP5* genes and infiltrating immune cells. *DPP6* was positively related to resting mast cells ($r = 0.570$, $p < 0.001$), monocytes ($r = 0.328$, $P = 0.032$) and activated dendritic cells ($r = 0.301$, $p = 0.0495$) but negatively related to eosinophils ($r = -0.321$, $P = 0.036$) and M0 macrophages ($r = -0.450$, $P = 0.003$) (Figure 7D). Moreover, *MFAP5* was positively related to resting mast cells ($r = 0.413$, $p = 0.006$) (Figure 7E). These findings supported that *DPP6* and *MFAP5* are related to immune activity.

Discussion

ULMS is one of the most common subtypes in mesenchymal neoplasms, but research on ULMS is limited. Because the incidence rate is low, different clinical features and histopathological appearances result in a lack of molecular biomarkers, offering no superior treatment regimen (21). The biological behaviour of ULMS is difficult to predict. Although the tumor is often restricted to the uterus, recurrence and metastasis are highly common (22). An increasing number of studies have employed immune cells as a new bioinformatic approach to investigate the diagnosis and prognosis of various diseases, including gastric cancer (23), breast cancer (24) and osteosarcoma (25). However, there are few studies on the immune cell infiltration association with DEGs in ULMS. Thus, we focused on the identification of significant diagnostic

DEGs for ULMS and determined the correlation of these DEGs with infiltrating immune cells in ULMS.

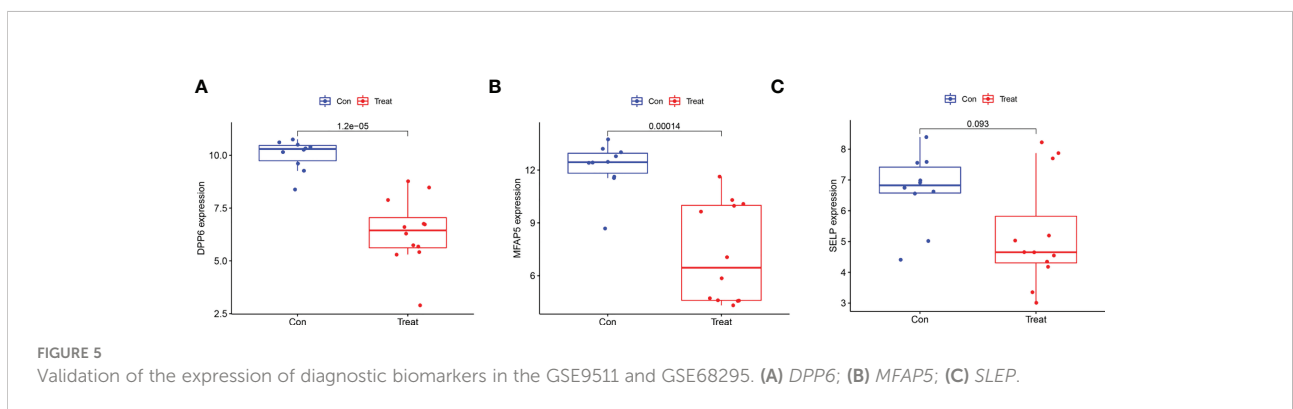
To our knowledge, our study is the first to apply multiple GEO datasets for knowledge mining using a machine learning approach in ULMS to identify significant diagnostic biomarkers related to immune cells. In the present study, which utilized the GSE36610, GSE64763, GSE9511 and GSE68295 datasets from the GEO database, 55 DEGs were identified by comparing ULMS and ULM samples. DO enrichment showed that the 55 DEGs were mainly related to solid malignant tumors and haematological malignancies. KEGG analysis and GSEA indicated that the DEGs were involved in regulating immune-related pathways and the cell cycle. Risinger et al. reported that defective postreplication mismatch repair resulting in microsatellite instability is present in considerable portions of sarcomas in gynecology (26). Similarly, mismatch repair (MMR) protein has been screened in uterine carcinosarcomas and leiomyosarcomas by immunohistochemical assays but has not been identified in other types of uterine mixed epithelial/mesenchymal or mesenchymal malignancies (27). Anderson et al. found that p53 expression may act as a prognostic biomarker for ULMS (28). Abnormal p53 staining (null or strong/diffuse) has been observed in ULMS with 70% sensitivity and 100% specificity against inflammatory myofibroblastic tumors (IMTs) and is related to genomic alterations (29). Relevant study has demonstrated that HTLV-1 infection correlates with the occurrence of ULMS. However, HTLV-1 has been thoroughly



studied in adult T-cell leukaemia/lymphoma (ATL) (30–32), an aggressive CD4+ T-cell malignancy. HTLV-1 increases genomic instability by directly altering the expression of host genes; conversely, abnormal gene expression may influence the longevity of infected CD4+ T cell clones and proliferation rate, allowing further mutations to accumulate and the host genome structure to vary, ultimately leading to malignant transformation

(33). Because HTLV-1 mediates immune-related pathways, it possible that regulation of the immune response is strongly associated with the occurrence of ULMS.

We identified two diagnostic biomarkers based on integrating two machine-learning algorithms and diagnostic ability analysis, and we verified these markers using the GSE9511 and GSE68295 datasets. The dipeptidyl peptidase 6



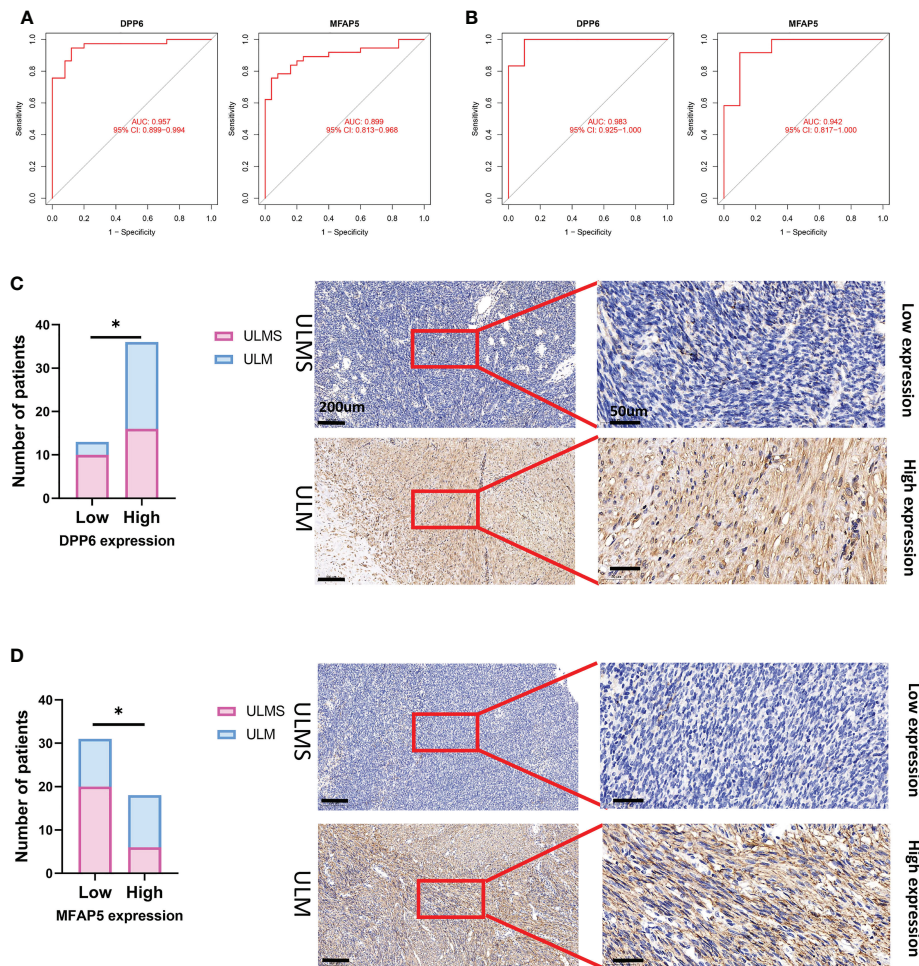
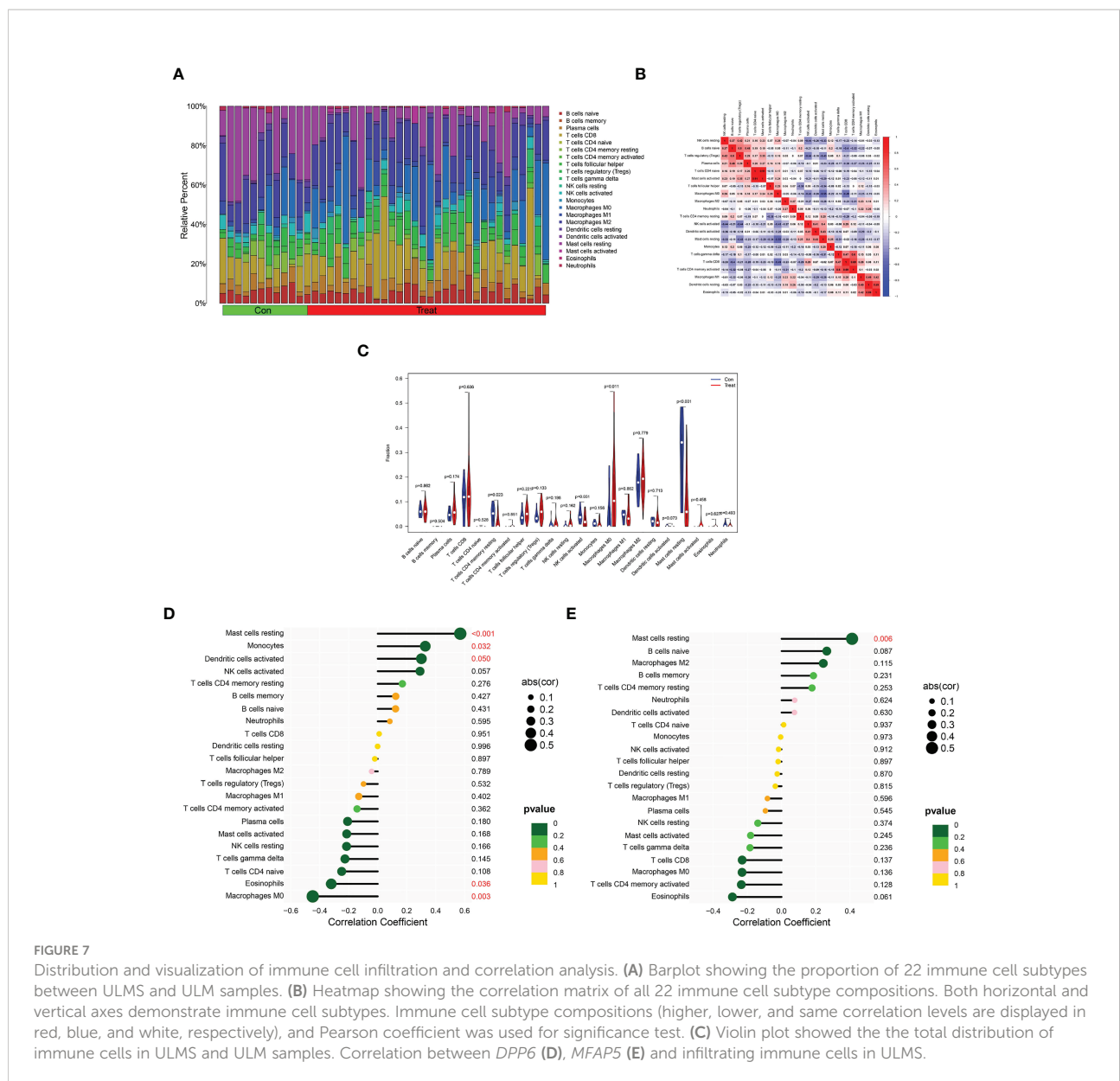


FIGURE 6

The receiver operating characteristic (ROC) curve of the diagnostic effectiveness of the six diagnostic markers. **(A)** ROC curve of *DPP6* and *MFAP5* after fitting to one variable in the metadata cohort; **(B)** ROC curve of *DPP6* and *MFAP5* after fitting to one variable in the GSE9511 and GSE68295 dataset. **(C)** Significantly low *DPP6* expression was observed in ULMS tissues compared with ULM specimens (ULMS=26, ULM=23). Representative images ($\times 50$ and $\times 400$) of IHC staining for *DPP6* in 26 ULMS and 23 ULM patients (high expression vs. low expression). **(D)** Significantly low *MFAP5* expression was observed in ULMS tissues compared with ULM specimens (ULMS=26, ULM=23). Representative images ($\times 50$ and $\times 400$) of IHC staining for *MFAP5* in 26 ULMS and 23 ULM patients (high expression vs. low expression). Scale bars are shown. * $P < 0.05$. P values were calculated by chi-square tests.

(*DPP6*) gene encodes a single transmembrane peptidase without activity. Most likely, *DPP6* enhances its expression and regulates its gating feature by combining at the permeation and gating modules of the potassium channel (34). In breast cancer tissues, *DPP6* has low expression at the transcription and protein levels, and in breast cancer patients, low expression of *DPP6* indicates poor prognoses, suggesting that *DPP6* may serve as a tumour suppressor in tumour development (35), which agreed with our study. However, in surgically treated clear cell renal cell carcinoma (ccRCC) patients, the promoter methylation of *DPP6* genes is related to an aggressive phenotype and early progression of distant metastasis (36). Similarly, in pancreatic ductal adenocarcinoma tissues, the promoter methylation of

DPP6 genes is significantly higher than that in normal tissues (37). Microfibril-associated protein 5 (*MFAP5*) is a 25 kDa glycoprotein present in the extracellular matrix and stroma in all tissues (38), and it is crucial for elastic microfibril assembly. Using a microarray to investigate prostate tumors, researchers have detected 3800 significant expression alterations between the tumor stroma and benign stroma, and they reported that the downregulation of *MFAP5* expression is the most significant alteration in the prostate cancer stroma among all genes examined (39). Significant loss of *MFAP5* expression in colon cancer stroma may facilitate the difference between pseudoinvasive and true invasive tumors with a specificity of 75% and a sensitivity of 80% in colonic adenomatous polyps



(40). However, high expression levels of *MFAP5* are associated with a worse prognosis in ovarian cancer (both in epithelium and stroma). In the present study, we observed significantly low expression of *MFAP5* in the stromal component of ULMS specimens, similar to the above study.

We applied CIBERSORT to assess the types of immune cell infiltration in ULMS and ULM. We discovered that decreased infiltration of resting CD4+ memory T cells, activated NK cells and resting mast cells in addition to increased infiltration of M0 macrophages were potentially correlated with the occurrence and development of ULMS. Xiaoqing et al. found that the infiltration of two types of immune cells (resting mast cells resting and activated NK cells) is lower in ULMS tissues, while the infiltration of five types of immune cells (memory B cells, M0

macrophages, activated mast cells, M1 macrophages and follicular helper T cells) is higher in ULMS tissues than in normal myometrium (NL) tissues (41). Similarly, our study demonstrated that the infiltration of immune cell types was lower due to the selection of the control group. Additionally, we found that the *DPP6* gene was positively correlated with resting mast cells, monocytes and activated dendritic cells. However, M0 macrophages and eosinophils had a negative correlation with the *DPP6* gene. Together, these findings indicated that the *DPP6* gene is associated with several types of immune cell infiltration and plays an important role in ULMS, suggesting that should be a focus in future experimental work.

The present study had limitations. First, due to the low incidence rate of ULMS, the number of cases was not enough in

the GSE36610 and GSE64763 datasets. Second, the function and reproducibility of the *DPP6* and *MFAP5* genes as well as the related immune cell infiltration should be further validated by prospective studies with larger sample sizes in ULMS.

Conclusion

Based on the GEO database, the two hub genes and the infiltration of five types of immune cells were related to ULMS occurrence. *DPP6* and *MFAP5* genes may affect the occurrence of ULMS through immune-related pathways. Thus, these findings provided molecular evidence for the treatment of ULMS in the future.

Data availability statement

The original contributions presented in the study are included in the article/Supplementary Material. Further inquiries can be directed to the corresponding author.

Ethics statement

The studies involving human participants were reviewed and approved by Ethics committee of The Second Affiliated Hospital of Fujian Medical University. The patients/participants provided their written informed consent to participate in this study.

Author contributions

All authors contributed to the article and approved the submitted version.

References

- Kobayashi H, Uekuri C, Akasaka J, Ito F, Shigemitsu A, Koike N, et al. The biology of uterine sarcomas: A review and update. *Mol Clin Oncol* (2013) 1:599–609. doi: 10.3892/mco.2013.124
- Ricci S, Stone RL, Fader AN. Uterine leiomyosarcoma: Epidemiology, contemporary treatment strategies and the impact of uterine morcellation. *Gynecol Oncol* (2017) 145:208–16. doi: 10.1016/j.ygyno.2017.02.019
- George S, Serrano C, Hensley ML, Ray-Coquard I. Soft tissue and uterine leiomyosarcoma. *J Clin Oncol* (2018) 36:144–50. doi: 10.1200/JCO.2017.75.9845
- D'Ambrosio L, Touati N, Blay JY, Grignani G, Flippot R, Czarnecka AM, et al. Doxorubicin plus dacarbazine, doxorubicin plus ifosfamide, or doxorubicin alone as a first-line treatment for advanced leiomyosarcoma: A propensity score matching analysis from the European organization for research and treatment of cancer soft tissue and bone sarcoma group. *Cancer* (2020) 126:2637–47. doi: 10.1002/cncr.32795. European Organization for Research and Treatment of Cancer Soft Tissue and Bone Sarcoma Group.
- Casali PG, Abecassis N, Aro HT, Bauer S, Biagini R, Bielack S, et al. Soft tissue and visceral sarcomas: ESMO-EURACAN clinical practice guidelines for diagnosis, treatment and follow-up. *Ann Oncol* (2018) 29:iv268–9. doi: 10.1093/annonc/mdy321
- Kapp DS, Shin JY, Chan JK. Prognostic factors and survival in 1396 patients with uterine leiomyosarcomas: emphasis on impact of lymphadenectomy and oophorectomy. *Cancer* (2008) 112:820–30. doi: 10.1002/cncr.23245
- Roberts ME, Aynardi JT, Chu CS. Uterine leiomyosarcoma: A review of the literature and update on management options. *Gynecol Oncol* (2018) 151:562–72. doi: 10.1016/j.ygyno.2018.09.010
- Mori KM, Abaid LN, Mendivil AA, Brown JV3rd, Beck TL, Micha JP, et al. The incidence of occult malignancy following uterine morcellation: A ten-year single institution experience retrospective cohort study. *Int J Surg* (2018) 53:239–42. doi: 10.1016/j.ijsu.2018.03.075
- Kaganov H, Ades A, Fraser DS. Preoperative magnetic resonance imaging diagnostic features of uterine leiomyosarcomas: A systematic review. *Int J Technol Assess Health Care* (2018) 34:172–9. doi: 10.1017/S0266462318000168
- Major FJ, Blessing JA, Silverberg SG, Morrow CP, Creasman WT, Currie JL, et al. Prognostic factors in early-stage uterine sarcoma. *cancer* (1993) 71:1702–9. doi: 10.1002/cncr.2820710440
- Marret H, Fritel X, Ouldamer L, Bendifallah S, Brun JL, De Jesus I, et al. And cngof, therapeutic management of uterine fibroid tumors: updated French

Funding

This work was supported by the Fujian Provincial Health Technology Project (No. 2019-1-15).

Acknowledgments

The authors acknowledge the GEO database for providing data of ULMS and ULM available.

Conflict of interest

The authors declare that the research was conducted in the absence of any commercial or financial relationships that could be construed as a potential conflict of interest.

Publisher's note

All claims expressed in this article are solely those of the authors and do not necessarily represent those of their affiliated organizations, or those of the publisher, the editors and the reviewers. Any product that may be evaluated in this article, or claim that may be made by its manufacturer, is not guaranteed or endorsed by the publisher.

Supplementary material

The Supplementary Material for this article can be found online at: <https://www.frontiersin.org/articles/10.3389/fonc.2022.1084192/full#supplementary-material>

- guidelines. *Eur J Obstet Gynecol Reprod Biol* (2012) 165:156–64. doi: 10.1016/j.ejogrb.2012.07.030
12. D'Angelo E, Prat J. Uterine sarcomas: A review. *Gynecol Oncol* (2010) 116:131–9. doi: 10.1016/j.ygyno.2009.09.023
13. Pritts EA, Vanness DJ, Berek JS, Parker W, Feinberg R, Feinberg J, et al. The prevalence of occult leiomyosarcoma at surgery for presumed uterine fibroids: a meta-analysis. *Gynecol Surg* (2015) 12:165–77. doi: 10.1007/s10397-015-0894-4
14. Giraldo NA, Becht E, Remark R, Damotte D, Sautes-Fridman C, Fridman WH. The immune contexture of primary and metastatic human tumours. *Curr Opin Immunol* (2014) 27:8–15. doi: 10.1016/j.coi.2014.01.001
15. Wu J, Zhao Y, Zhang J, Wu Q, Wang W. Development and validation of an immune-related gene pairs signature in colorectal cancer. *Oncoimmunology* (2019) 8:1596715. doi: 10.1080/2162402X.2019.1596715
16. Zhao E, Zhou C, Chen S. A signature of 14 immune-related gene pairs predicts overall survival in gastric cancer. *Clin Transl Oncol* (2021) 23:265–74. doi: 10.1007/s12094-020-02414-7
17. Leek JT, Johnson WE, Parker HS, Jaffe AE, Storey JD. The sva package for removing batch effects and other unwanted variation in high-throughput experiments. *Bioinformatics* (2012) 28:882–3. doi: 10.1093/bioinformatics/bts034
18. Guyon I, Weston J, Barnhill S, Vapnik V. Gene selection for cancer classification using support vector machines. *Machine Learn.* (2002) 46:389–422. doi: 10.1023/A:1012487302797
19. Newman AM, Liu CL, Green MR, Gentles AJ, Feng W, Xu Y, et al. Robust enumeration of cell subsets from tissue expression profiles. *Nat Methods* (2015) 12:453–7. doi: 10.1038/nmeth.3337
20. Chen H, Wang J, Yang H, Chen D, Li P. Association between FOXM1 and hedgehog signaling pathway in human cervical carcinoma by tissue microarray analysis. *Oncol Lett* (2016) 12:2664–73. doi: 10.3892/ol.2016.4932
21. Tsuyoshi H, Yoshida Y. Molecular biomarkers for uterine leiomyosarcoma and endometrial stromal sarcoma. *Cancer Sci* (2018) 109:1743–52. doi: 10.1111/cas.13613
22. Desar IME, Ottevanger PB, Benson C, van der Graaf WTA. Systemic treatment in adult uterine sarcomas. *Crit Rev Oncol Hematol* (2018) 122:10–20. doi: 10.1016/j.critrevonc.2017.12.009
23. Xiang A, Lin X, Xu L, Chen H, Guo J, Zhou F. PCOLCE is potent prognostic biomarker and associates with immune infiltration in gastric cancer. *Front Mol Biosci* (2020) 7:544895. doi: 10.3389/fmolb.2020.544895
24. Yao S, Cheng TD, Elkhanany A, Yan L, Omilian A, Abrams SI, et al. Breast tumor microenvironment in black women: A distinct signature of CD8+ T-cell exhaustion. *J Natl Cancer Inst* (2021) 113:1036–43. doi: 10.1093/jnci/djaa215
25. Zheng J-H, Zhang C, Lin Z-H, Lv H-Y, Ye Z-M, Chen Y-P, et al. Profiles of immune cell infiltration and immune-related genes in the tumor microenvironment of osteosarcoma. *Aging* (2020) 12:3486–501. doi: 10.18632/aging.102824
26. Risinger JJ, Boyer JC, Evans AC, Berchuck A, Kunkel TA, Barrett JC. Microsatellite instability in gynecological sarcomas and in hMSH2 mutant uterine sarcoma cell lines defective in mismatch repair activity. *Cancer Res* (1995) 55:5664–9.
27. Hoang LN, Ali RH, Lau S, Gilks CB, Lee CH. Immunohistochemical survey of mismatch repair protein expression in uterine sarcomas and carcinosarcomas. *Int J Gynecol Pathol* (2014) 33:483–91. doi: 10.1097/PGP.0b013e31829ff239
28. Anderson SE, Chuai S, Olshen AB, D. CHI, Sabbatini P, Soslow RA. p53, epidermal growth factor, and platelet-derived growth factor in uterine leiomyosarcoma and leiomyomas. *Int J Gynecol Cancer* (2006) 16:849–53. doi: 10.1111/j.1525-1438.2006.00542.x
29. Schaefer IM, Hornick JL, Sholl LM, Quade BJ, Nucci MR, Parra-Herran C. Abnormal p53 and p16 staining patterns distinguish uterine leiomyosarcoma from inflammatory myofibroblastic tumour. *Histopathology* (2017) 70:1138–46. doi: 10.1111/his.13176
30. Kannagi M, Hasegawa A, Nagano Y, Kimpara S, Suehiro Y. Impact of host immunity on HTLV-1 pathogenesis: potential of tax-targeted immunotherapy against ATL. *Retrovirology* (2019) 16:23. doi: 10.1186/s12977-019-0484-z
31. Kannagi M, Ohashi T, Harashima N, Hanabuchi S, Hasegawa A. Immunological risks of adult T-cell leukemia at primary HTLV-I infection. *Trends Microbiol* (2004) 12:346–52. doi: 10.1016/j.tim.2004.05.005
32. Matsuoka M. Human T-cell leukemia virus type I (HTLV-I) infection and the onset of adult T-cell leukemia (ATL). *Retrovirology* (2005) 2:27. doi: 10.1186/1742-4690-2-27
33. Cook L, Melamed A, Yaguchi H, Bangham CR. The impact of HTLV-1 on the cellular genome. *Curr Opin Virol* (2017) 26:125–31. doi: 10.1016/j.coviro.2017.07.013
34. Kaulin YA, De Santiago-Castillo JA, Rocha CA, Nadal MS, Rudy B, Covarrubias M. The dipeptidyl-peptidase-like protein DPP6 determines the unitary conductance of neuronal Kv4.2 channels. *J Neurosci* (2009) 29:3242–51. doi: 10.1523/JNEUROSCI.4767-08.2009
35. Choy TK, Wang CY, Phan NN, Khoa Ta HD, Anuraga G, Liu YH, et al. Identification of dipeptidyl peptidase (DPP) family genes in clinical breast cancer patients via an integrated bioinformatics approach. *Diagnostics (Basel)* (2021) 11(7):1204. doi: 10.3390/diagnostics11071204
36. Kang HW, Park H, Seo SP, Byun YJ, Piao XM, Kim SM, et al. Methylation signature for prediction of progression free survival in surgically treated clear cell renal cell carcinoma. *J Korean Med Sci* (2019) 34:e144. doi: 10.3346/jkms.2019.34.e144
37. Zhao X, Cao D, Ren Z, Liu Z, Lv S, Zhu J, et al. Dipeptidyl peptidase like 6 promoter methylation is a potential prognostic biomarker for pancreatic ductal adenocarcinoma. *Biosci Rep* (2020) 40(7):BSR20200214. doi: 10.1042/BSR20200214
38. Uhlen M, Fagerberg L, Hallstrom BM, Lindskog C, Oksvold P, Mardinoglu A, et al. Proteomics. tissue-based map of the human proteome. *Science* (2015) 347:1260419. doi: 10.1126/science.1260419
39. Jia Z, Wang Y, Sawyers A, Yao H, Rahmatpanah F, Xia XQ, et al. Diagnosis of prostate cancer using differentially expressed genes in stroma. *Cancer Res* (2011) 71:2476–87. doi: 10.1158/0008-5472.CAN-10-2585
40. Zhao L, Westerhoff M, Hornick JL, Krausz T, Antic T, Xiao SY, et al. Loss of microfibril-associated protein 5 (MFAP5) expression in colon cancer stroma. *Virchows Arch* (2020) 476:383–90. doi: 10.1007/s00428-019-02649-y
41. Shen X, Yang Z, Feng S, Li Y. Identification of uterine leiomyosarcoma-associated hub genes and immune cell infiltration pattern using weighted co-expression network analysis and CIBERSORT algorithm. *World J Surg Oncol* (2021) 19:223. doi: 10.1186/s12957-021-02333-z